Generating finite element method in constructing complex-shaped multigrid finite elements

Aleksandr Matveev[1,*]

[1]ICM SB RAS, 50, bil. 44, Akademgorodok, Krasnoyarsk, Russia, 660036

Abstract. The calculations of three-dimensional composite bodies based on the finite element method with allowance for their structure and complex shape come down to constructing high-dimension discrete models. The dimension of discrete models can be effectively reduced by means of multigrid finite elements (MgFE). This paper proposes a generating finite element method for constructing two types of three-dimensional complex-shaped composite MgFE, which can be briefly described as follows. An MgFE domain of the first type is obtained by rotating a specified complex-shaped plane generating single-grid finite element (FE) around a specified axis at a given angle, and an MgFE domain of the second type is obtained by the parallel displacement of a generating FE in a specified direction at a given distance. This method allows designing MgFE with one characteristic dimension significantly larger (smaller) than the other two. The MgFE of the first type are applied to calculate composite shells of revolution and complex-shaped rings, and the MgFE of the second type are used to calculate composite cylindrical shells, complex-shaped plates and beams. The proposed MgFE are advantageous because they account for the inhomogeneous structure and complex shape of bodies and generate low-dimension discrete models and solutions with a small error.

1 Introduction

The finite element method (FEM) [1, 2] is widely used to study the stress-strain state (SSS) of complex-shaped elastic composite bodies. In order to simplify calculations, the deformation of bodies of a certain type (for example, beams, plates, shells) is described using engineering theories based on hypotheses [3–9]. However, engineering solutions do not always meet modern requirements. Calculating composite bodies on the basis of the FEM in the formulation of a three-dimensional problem of the elasticity theory [10] with account for their structure can be reduced to constructing high-dimension discrete models, of the order of $10^9 \div 10^{12}$. For such discrete models, it is difficult to use computational software such as ANSYS, NASTRAN, etc. [2]. The dimension of discrete models can be effectively reduced by means of the MgFE [11–18], which also serve as a basis for the multigrid finite element method (MFEM) [13–17], based on the FEM

[*] Corresponding author: mtv241@mail.ru

© The Authors, published by EDP Sciences. This is an open access article distributed under the terms of the Creative Commons Attribution License 4.0 (http://creativecommons.org/licenses/by/4.0/).

algorithms. The main advantages and features distinguishing the MFEM from the FEM are as follows.

1. In the MFEM (without increasing the dimension of MgFE), one can use arbitrarily small basic partitions of bodies, i.e., MgFE, which allows one to arbitrarily accurately account for their complex shape and inhomogeneous structure, as well as the complex nature of fixing and loading bodies. In the FEM, it is impossible to use arbitrarily small basic partitions because the PC resources are limited, which means that the MFEM is more effective than the FEM.

2. Application the MFEM (based on the basic models of bodies) requires a significantly smaller amount of RAM ($10^3 \div 10^6$ times) and time compared to the FEM used for basic models, i.e., the MFEM is more economical than FEM.

3. The MFEM uses homogeneous and composite MgFE constructed using nested grids, which expands the field of application of this method. The FEM uses single-grid homogeneous finite elements (FE). It is noteworthy that boundary-value problems can always be solved using the MFEM instead of the FEM because MgFE can always be used instead of single-grid FE. As *m*gFE are constructed using *m* nested grids instead of one (*m*>1), the MFEM can be regarded as the generalization of the FEM, i.e., the FEM is a special case of the MFEM. Hence, if the FEM-based calculations of bodies are carried out using MgFE, then this case is essentially the implementation of the MFEM.

In this paper, the two types of complex-shaped three-dimensional composite MgFE are designed using the generating FEM. According to this method, the MgFE domain is obtained using the specified displacement of a given complex-shaped plane single-grid FE (below referred to as a generating FE) in a three-dimensional space. The MgFE domain of the first type is obtained by rotating the generating FE around a specified axis at a specified (small) angle, and the MgFE domain of the second type is obtained by the parallel displacement of the generating FE along a specified straight line at a given distance. The nodes of the generating FE are the nodes of a coarse grid of the MgFE, and the nodes of any cross section of the coarse grid of the MgFE are the nodes of the generating FE. This approach simplifies the construction of approximating displacement functions on the coarse grids of the complex-shaped MgFE, where the basis functions of the generating FE are used, and Lagrange polynomials are applied along the direction of the generating FE. The MgFE of the first type are used to calculate the composite shells of revolution, and the MgFE of the second type are used to calculate the composite cylindrical shells of revolution (with a variable curvature radius) and complex-shaped plates and beams. It is assumed that there are ideal bonds between the components of the inhomogeneous structure of the MgFE. The calculation of composite shells of double curvature using the MgFE of the first type is described in [16], and the application of the MgFE of the first and second types for determining the power elements of standard designs is demonstrated in [18].

2 Multigrid FE of the first type. Complex-shaped composite shells of revolution

The fundamental principles of constructing the MgFE of the first type, applied to analyze a three-dimensional SSS of composite shells of revolution, are considered on the example of a complex-shaped shell two-grid FE (2gFE), Fig. 1. For the V_d 2gFE, the following local coordinate systems are introduced: Cartesian $Oxyz$, curvilinear $O\xi\eta\zeta$, and integer ijk for the nodes of the coarse grid H_d of the 2gFE. The nodes of the H_d grid for the 2gFE are 36 in number and marked by dots in Fig. 1, with cd denoting the shell axis. The generating single-grid FE (1gFE) V_d^a for the V_d 2gFE has 12 nodes of the coarse grid H_d, denoted by dots in Fig. 2. The lateral sides of the V_d^a 1gFE are parallel and extended by a dotted line to an the intersection with the cd axis. The V_d 2gFE domain is obtained by rotating the generating complex-shaped 1gFE V_d^a around the cd axis at the specified angle α_0 (corresponding to partitioning the shell into 2gFE), and α_0 is the apex angle of the V_d 2gFE. The basic partition R_d of the V_d 2gFE comprises three homogeneous V_e 1gFE of the first order (described in detail in [12]), $e=1,...,M$, and M is the overall number of the V_e FE. The partition R_d accounts for the inhomogeneous structure and shape of the 2gFE and forms a fine grid h_d, where $H_d \subset h_d$. It is noteworthy that some nodes of the coarse grids of the MgFE can generally fail to match the nodes of the fine grids. We construct the V_e 1gFE by using the equations of the three-dimensional problem of the elasticity theory [10], written in the local Cartesian coordinate system of the V_e FE [12]. Thus, a three-dimensional SSS is implemented in the 2gFE. Radii R_1 and R_3 (R_2 and R_4) describe the bottom (top) boundaries of the lateral edges of the 2gFE. In the H_d grid, the displacements functions u_d, v_d, and w_d, used to reduce the dimension of the basic partition R_d, are calculated.

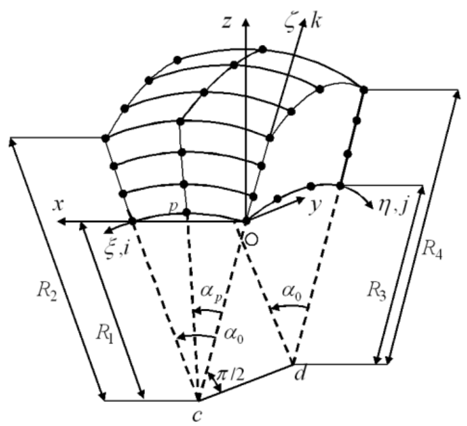

Fig. 1. Shell 2gFE V_d.

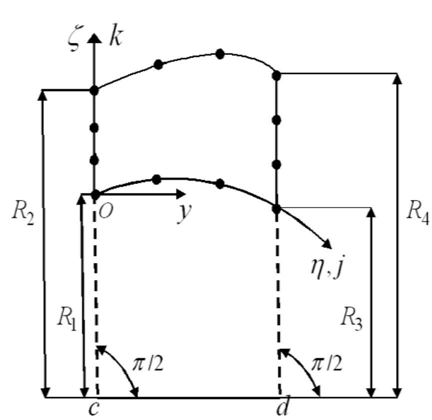

Fig. 2. Generating 1gFE V_d^a.

The basis function ψ_{ijk} for the i,j,k node of the coarse grid H_d of the V_d 2gFE is sought in the form

$$\psi_{ijk}(\alpha,y,\zeta)=N_{jk}(y,\zeta)L_i(\alpha)\,, \tag{1}$$

where $N_{jk}(y,\zeta)$ denotes the basis functions of the j,k node of the V_d^a 1gFE, corresponding to the polynomial $P_d(y,\zeta)$ of the form [2]

$P_d = a_1 + a_2 y + a_3\zeta + a_4 y\zeta + a_5 y^2 + a_6\zeta^2 + a_7 y^2\zeta + a_8 y\zeta^2 +$
$a_9 y\zeta^3 + a_{10} y^3\zeta + a_{11} y^3 + a_{12}\zeta^3$, $j,k=1,...,4$, $L_i(\alpha)$ is the second-order Lagrange polynomial, $L_i(\alpha)=\prod_{p=1,\,p\neq i}^{3}\dfrac{\alpha-\alpha_p}{\alpha_i-\alpha_p}$, where α_p (α_i) is the apex angle of the p node (i node), $i=1,...,3$, Fig. 1, and α is the apex angle of the M point lying in the V_d 2gFE domain.

Thus, the basis functions ψ_{ijk} of the V_d 2gFE of the first type are represented by power polynomials, which are the shape functions of the generating FE V_d^a, and by the Lagrange polynomials in the direction of rotation of the generating FE around the specified axis.

Denotations $N_\beta = \psi_{ijk}$, where $i = 1,...,3$; $j,k = 1,...,4$; $\beta = 1,...,36$. Then, using (1), we write the displacement functions u_d, v_d, and w_d as

$$u_d = \sum_{\beta=1}^{36} N_\beta u_\beta , \quad v_d = \sum_{\beta=1}^{36} N_\beta v_\beta , \quad w_d = \sum_{\beta=1}^{36} N_\beta w_\beta , \tag{2}$$

where N_β, u_β, v_β, and w_β denote the basis function and displacements of the β-th node of the H_d grid.

The functional of the total potential energy Π_d of the base partition R_d of the 2gFE is written in the form

$$\Pi_d = \sum_{e=1}^{M} (\frac{1}{2} \boldsymbol{\delta}_e^T [K_e] \boldsymbol{\delta}_e - \boldsymbol{\delta}_e^T \mathbf{P}_e) , \tag{3}$$

where $[K_e]$, $\mathbf{P}_e$, and $\boldsymbol{\delta}_e$ denote the stiffness matrix, nodal force vectors, and displacement vectors of the V_e 1gFE, corresponding to the coordinate system *Oxyz* of the V_d 2gFE.

Equations (2) are used to express the nodal displacement vector $\boldsymbol{\delta}_e$ of the base 1gFE V_e through the nodal displacement vector $\boldsymbol{\delta}_d$ of the coarse grid H_d ($\boldsymbol{\delta}_d = \{u_\beta, v_\beta, w_\beta\}^T$), i.e.

$$\boldsymbol{\delta}_e = [A_e^d] \boldsymbol{\delta}_d , \tag{4}$$

where $[A_e^d]$ denotes the rectangular matrix, $e = 1,..., M$.

Equation (4) is substituted into Eq. (3) and the condition $\partial \Pi_d (\boldsymbol{\delta}_d) / \partial \boldsymbol{\delta}_d = 0$ yields the relationship $[K_d] \boldsymbol{\delta}_d = \mathbf{F}_d$, where

$$[K_d] = \sum_{e=1}^{M} [A_e^d]^T [K_e][A_e^d] , \quad \mathbf{F}_d = \sum_{e=1}^{M} [A_e^d]^T \mathbf{P}_e . \tag{5}$$

Here $[K_d]$ is the stiffness matrix, and $\mathbf{F}_d$ is the nodal force vector of the 2gFE V_d .

Let the vector $\boldsymbol{\delta}_d$ be determined. Equation (4) is used to calculate vector $\boldsymbol{\delta}_e$ of the nodal displacements of the V_e 1gFE in the coordinate system *Oxyz* of the V_d 2gFE. The displacement vector $\boldsymbol{\delta}_e^*$ of the V_e 1gFE (corresponding to the local Cartesian coordinate system of the V_e 1gFE) is sought for by the expression $\boldsymbol{\delta}_e^* = [M_e] \boldsymbol{\delta}_e$, where $[M_e]$ is the rotation matrix [2]. The vector $\boldsymbol{\delta}_e^*$ and the known algorithms of the FEM [1, 2] are used to calculate the equivalent stress at the center of the V_e 1gFE domain.

The calculations of the elastic composite round cylindrical shells and panels, carried out using MgFE, are described in [12]. The base functions of the coarse grids of the 2gFE of these shells are determined in the form of Lagrange polynomials and using the power polynomials $P(x, y, z)$ of the first, second, and third orders [12], written in the local Cartesian coordinate systems. The MgFE of the shells of revolution are verified using the known numerical method [2, 12].

Note 1. In view of Eq. (4), the dimension of the vector $\boldsymbol{\delta}_d$ (i.e., the dimension of V_d 2gFE) is independent of M , which is the total number of the base FE V_e that comprise the

V_d 2gFE domain. Consequently, it is possible to use arbitrarily small basic partitions R_d, allowing one to arbitrarily exactly account for the complex shape and inhomogeneous (microinhomogeneous) structure of the 2gFE V_d and its complex fixing and loading, as well as to arbitrarily exactly describe a three-dimensional SSS in the V_d 2gFE domain (with no increase in the dimension of the V_d 2gFE, which is noteworthy).

As shown by the calculations, as the basic partitions of the MgFE become finer, the solution errors decrease. Similarly, the procedures described in Sec. 2 are used to design the composite 2gFE for calculating complex-shaped composite rings and shafts with central circular holes. Three-grid FE (3gFE) of the first type are designed using the 2gFE of the first type with the help of procedures similar to those in Sec. 2

You are free to use colour illustrations for the online version of the proceedings but any print version will be printed in black and white unless special arrangements have been made with the conference organiser. Please check whether or not this is the case. If the print version will be black and white only, you should check your figure captions carefully and remove any reference to colour in the illustration and text. In addition, some colour figures will degrade or suffer loss of information when converted to black and white, and this should be taken into account when preparing them.

3 Multigrid FE of the second type

3.1 Multigrid FE for calculating complex-shaped composite beams

The main provisions of the construction procedure for the MgFE of the second type used to analyze the three-dimensional SSS of composite beams are considered on the example of the V_p 2gFE (Fig. 3), which is a complex-shaped rectilinear composite beam with a hole, with the hole section hatched in the figure. The domain of the V_p 2gFE is obtained by the parallel displacement of the generating complex-shaped 1gFE V_p^a (Fig. 4) with a hole (hatched) along the Oy axis at the specific distance d. The basic partition R_p of the V_p 2gFE consists of the homogeneous 1gFE V_e of the first order, $e = 1,..., M$. The partition R_p accounts for the inhomogeneous structure and complex shape of the V_p 2gFE and forms a fine grid h_p, in which the coarse grid H_p of the 2gFE is nested, and the nodes of the H_p grid are marked by points (48 nodes, Fig. 3). The stress state in the V_e 1gFE is described by the equations of the three-dimensional problem of the elasticity theory [10], written in the local Cartesian coordinate system of the V_e FE. Consequently, a three-dimensional SSS is implemented in the V_p 2gFE domain. The nodes of the V_p^a 1gFE of the third order are the nodes of the coarse grid H_p, marked by points (12 nodes). For the nodes of the H_p grid, a coordinate system ijk is introduced, in which $i, j, k = 1,..., 4$.

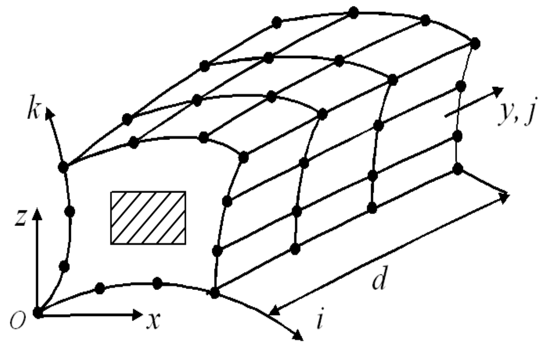

Fig. 3. Beam 2gFE V_p.

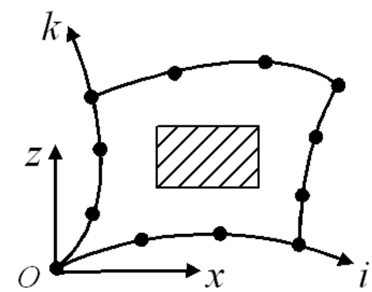

Fig. 4. Generating 1gFE V_p^a.

The basis function ψ_{ijk} for the i, j, k node of the coarse grid H_p is determined as

$$\psi_{ijk}(x, y, z) = N_{ik}(x, z)L_j(y), \tag{6}$$

where N_{ik} denotes the basis function of the i, k node of the generating FE V_p^a, corresponding to a polynomial of the form [2]

$$P(x, z) = a_1 + a_2x + a_3z + a_4xz + a_5x^2 + a_6z^2 + a_7x^2z + a_8xz^2 +$$

$$a_9xz^3 + a_{10}x^3z + a_{11}x^3 + a_{12}z^3, \tag{7}$$

$i, k = 1,\ldots,4$, $L_j(y)$ is the Lagrange polynomial of the third order, having the form

$$L_j(y) = \prod_{p=1, p\neq j}^{3} \frac{y - y_p}{y_j - y_p}, \tag{8}$$

where $j = 1,\ldots,4$, y_p is the coordinate of the node p of the coarse grid H_p, lying on the Oy axis (Fig. 3). Using Eq. (6), we write the displacement functions u_p, v_p, and w_p for the H_p grid in the form

$$u_p = \sum_{\beta=1}^{48} N_\beta u_\beta, \quad v_p = \sum_{\beta=1}^{48} N_\beta v_\beta, \quad w_p = \sum_{\beta=1}^{48} N_\beta w_\beta, \tag{9}$$

where u_p, v_p, and w_p denote the displacements of the β-th node of the coarse grid H_p, where $\beta = 1,...,48$.

It is noteworthy that the displacement functions u_p, v_p, and w_p are only used to reduce the dimension of the basic partition R_p of the V_p 2gFE. The displacement functions (9) and algorithms similar to those in Sec. 2 are used to determine the stiffness matrix and the nodal force vector of the V_p 2gFE of the second type.

Note 2. The proposed method allows designing 2gFE whose one characteristic dimension is significantly larger or smaller than all the others. In the Oy direction of the large dimension of the V_p 2gFE, it is reasonable to use the high order of displacement approximation (i.e., the high order of the Lagrange polynomials $L_j(y)$), which allows constructing solutions with a small error

3.2 Multigrid FE for calculating complex-shaped composite cylindrical shells

The construction procedure of the 2gFE of the second type, used to analyze the three-dimensional SSS of cylindrical shells of an inhomogeneous structure and complex shape, is considered on the example of the V_e^a 2gFE with characteristic dimensions of $17h \times 24h \times 18h$ (Fig. 5), which has a hole and the section of which is hatched in the figure. The generatrix (straight line) of the median surface of the V_e^a 2gFE is parallel to the Oy axis (Fig. 5). The V_e^a 2gFE domain is obtained by the parallel displacement of the generating complex-shaped 1gFE V_a (Fig. 6) (the hole section is hatched) along the Oy axis at a specified distance $d = 24h$. The basic partition R_a of the V_e^a 2gFE consists of cube-shaped homogeneous 1gFE V_e of the first order with side h, $e = 1,..., M$, where M denotes the total number of the V_e FE. The partition R_a accounts for the inhomogeneous structure and complex shape of the V_e^a 2gFE and forms a fine grid h_a, in which the coarse grid H_a of the 2gFE is nested ($H_a \subset h_a$). The nodes of the coarse grid H_a are marked in Fig. 5 by points (60 nodes). The nodes of the V_a 1gFE of the third order are the nodes of the coarse grid H_a, marked by points (12 nodes, Fig. 6). A stress state in the V_e 1gFE is described by the equations of the three-dimensional problem of the elasticity theory [10] (written in the local Cartesian coordinate system of the V_e FE). Consequently, the three-dimensional SSS is implemented in the V_e^a 2gFE domain.

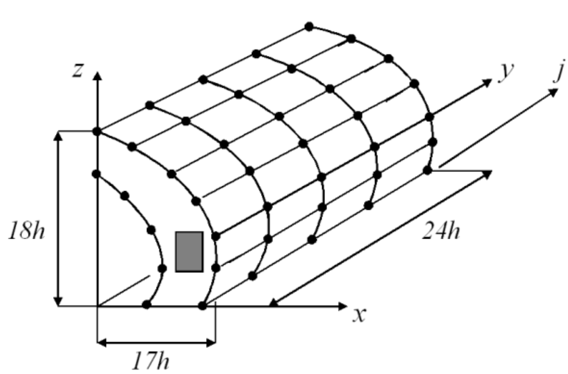

Fig. 5. V_e^a 2gFE.

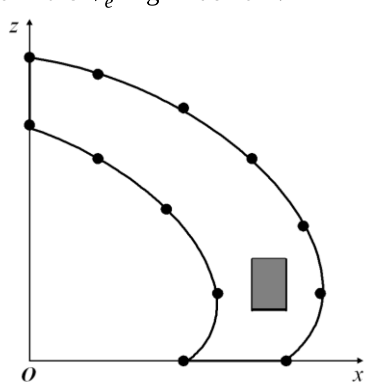

Fig. 6. Generating 1gFE V_a.

For the pair of numbers i, j, where $i = 1,...,12$, $j = 1,\ldots,5$, we determine an integer $\beta \geq 1$, $\beta = 1,\ldots,60$. The basis function $\psi_\beta(x, y, z)$ for the β-th node in the coarse grid of the V_e^a 2gFE is sought in the form

$$\psi_\beta(x, y, z) = N_i(x, z) L_j(y), \tag{10}$$

where $\beta = \overline{1,60}$, $N_i(x, z)$ is the shape function of the i th node of the generating 1gFE V_a, $i = 1,...,12$, corresponding to the polynomial $P(x, z)$, presented in the local Cartesian coordinate system Oxz (Fig. 6), of the form (7), $L_j(y)$ is the fourth-order Lagrange polynomial (Eq. (8)), where $j = 1,\ldots,5$, y_p is the coordinate of the p node of the coarse grid H_a, lying on the j axis, which is parallel to the Oy axis (Fig. 5).

In Eq. (10), the basis functions ψ_β 2gFE V_e^a of the second type are represented by power polynomials, i.e., functions of the form $N_i(x,z)$ of the generating FE V_a, and by the Lagrange polynomials $L_j(y)$ in the direction of the generating FE (along the Oy axis). Using Eq. (10), we write the displacement functions u_a, v_a, and w_a for the coarse grid H_a as

$$u_a = \sum_{\beta=1}^{60} N_\beta u_\beta \,, \quad v_a = \sum_{\beta=1}^{60} N_\beta v_\beta \,, \quad w_a = \sum_{\beta=1}^{60} N_\beta w_\beta \,, \tag{11}$$

where N_β, u_β, v_β, and w_β denote the basis function and displacements of the β-th node of the H_a grid.

It is noteworthy that the displacement functions u_a, v_a, and w_a are only used to reduce the dimension of the basic partition R_a of the 2gFE V_e^a. We use the displacement functions (11) and the algorithms similar to those in Sec. 2 to determine the stiffness matrix and the nodal force vector of the V_e^a 2gFE of the second type.

3.3 Multigrid FE for calculating complex-shaped composite plates

We consider the construction procedure for the 2gFE of the second type in order to analyze the three-dimensional SSS of plates with an inhomogeneous structure on the example of the complex-shaped composite laminated 2gFE V_g^b (Fig. 7), where $Oxyz$ is the Cartesian coordinate system. The characteristic dimensions B and H of the V_g^b 2gFE significantly exceed the dimension of h, with h being the thickness of the 2gFE. The V_g^b 2gFE domain is obtained by the parallel displacement of the generating 1gFE V_g (Fig. 8) along the Oy axis at the given distance h. The coarse grid of the V_g^b 2gFE has 27 nodes marked by points in Fig. 7. The basic partition of the V_g^b 2gFE consists of cube-shaped homogeneous FE of the first order (rectangular parallelepiped [2]), in which a three-dimensional SSS is implemented. It is noteworthy that the basic partitions of the 2gFE can be arbitrarily small, i.e., can arbitrarily exactly account for the inhomogeneous structure and complex shape of the 2gFE. The base function $\psi_\beta(x,y,z)$ for the β-th node in the coarse grid of the V_g^b 2gFE is sought in the form (6), where $\beta = 1,\ldots,27$, $N_i(x,z)$ is the shape function of the i-th node of the generating 1gFE V_g, $i = 1,\ldots,9$, corresponding to a polynomial of the form $P_g(x,z) = a_1 + a_2 x + a_3 z + a_4 xz + a_5 x^2 + a_6 z^2 + a_7 x^2 z + a_8 xz^2 + a_9 x^2 z^2$, presented in the local Cartesian coordinate system Oxz, Fig. 8, and $L_j(y)$ denotes the Lagrange polynomials of the second order.

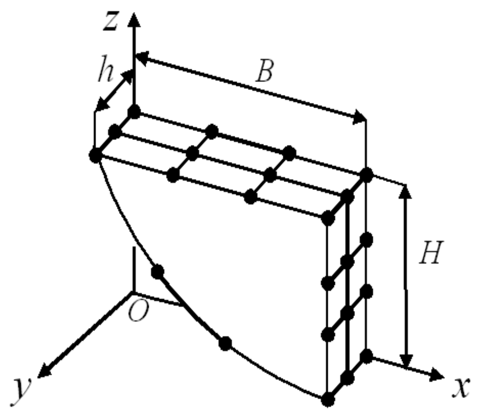

Fig. 7. Laminated 2gFE V_g^b.

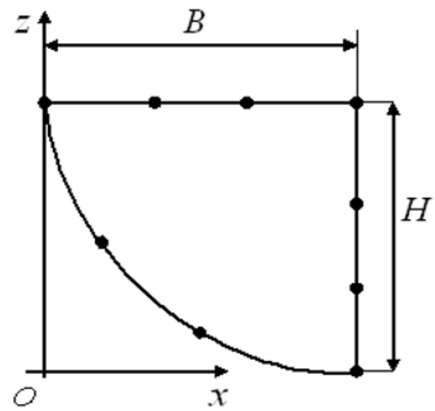

Fig. 8. Generating 1gFE V_g.

The stiffness matrix and nodal force vector of the laminated 2gFE V_g^b are determined using procedures similar to those in Secs. 3.1 and 3.2. The discrete models of the plates are generally comprised of complex-shaped 2gFE (such as curvilinear 2gFE V_g^b) and 2gFE shaped as a rectangular parallelepiped, constructed with the help of power polynomials [2], and Lagrange polynomials [12]. It is noteworthy that the proposed MgFE of the first and second types can be used in analyzing the three-dimensional SSS of corrugated plates, panels, and floors [19, 20] (corrugation can be shaped as a trapezium, rectangle, triangle, a part of a circular arc, etc.). Three-grid FE (3gFE) of the second type are designed using the 2gFE of the second type with the help of procedures similar to those in Secs. 2, 3.2, and 3.3.

3.4 Multigrid FE for calculating curvilinear composite beams

We consider a curvilinear beam l_1 (frame beam). The V_L^a 2gFE domain (Fig. 9), where the 2gFE approximates the beam l_1, is obtained by the parallel displacement of the generating 1gFE V_L (Fig. 10) along the Oy axis at the distance d, which is the beam width. The transverse section of the beam is $h \times d$, where h is its height (thickness), corresponding to arc ds (Fig. 9). The thickness of the transverse beam can be variable. The coarse grid of the V_L^a 2gFE has 24 nodes marked by points (Fig. 9).

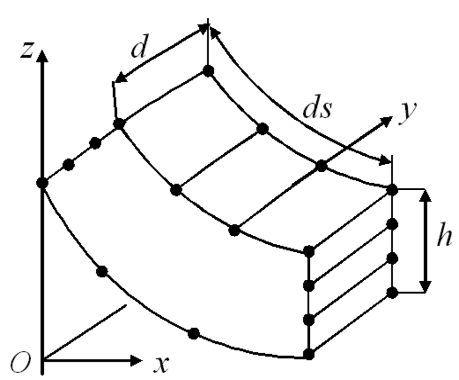

Fig. 9. Frame 2gFE V_L^a.

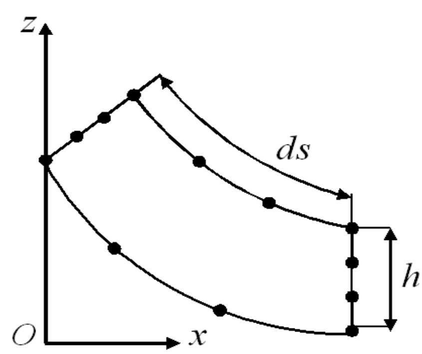

Fig. 10. Generating 1gFE V_L.

The basis function $\psi_\beta(x,y,z)$ for the β-th node of the coarse grid of the V_L^a 2gFE is determined in the form (10), where $\beta = 1,\ldots,24$, $N_i(x,z)$ denotes the shape function of the i-th node of the generating 1gFE V_L (Fig. 10), $i = 1,...,12$, corresponding to a polynomial of the form (7), written in the local Cartesian coordinate system Oxz (Fig. 10), and $L_j(y)$ denotes the Lagrange polynomials of the first order. $i = 1,...,12$. The stiffness matrix and nodal force vector of the V_L^a 2gFE are determined in procedures similar to those in Secs. 3.2 and 3.3.

4 Conclusion

In this paper, three-dimensional composite and homogeneous MgFE of two types of complex shapes are considered, which are designed with the use of forming FE. The procedures for the construction of type 1 and type 2 MgFE are described, which are used for the calculation of composite (homogeneous) shells of rotation, cylindrical shells (with a variable radius of curvature), plates and beams of complex shape. The main advantages of the proposed MgFE are that they take into account the inhomogeneous, micro-inhomogeneous structure and complex shape of bodies, describe three-dimensional behavior in composite (homogeneous) bodies, form discrete models of small dimension and generate approximate solutions with a small error.

References

1. O.C. Zienkiewicz. *The Finite Element Method in Engineering Science* (McGraw-Hill, London, 1971)
2. D.H. Norrie and G. de Vries. *An Introduction to Finite Element Analysis* (Academic Press, New York, San Francisco, London, 1978)
3. A.P. Kiselev, N.A. Gureeva, R.Z. Kiselyova, Izv. Vuzov. Stroitel'stvo, **1**, 106-112 (2010)
4. S.K. Golushko, Yu.V. Nemirovskii. *Direct and Inverse Problems of the Mechanics of Elastic Composite Plates and Shells of Revolution* (Fizmatlit, Moscow, 2008)
5. A. Ahmed A, S. Kapuria, Composite Structures, **158**, 112–127 (2016)
6. E. Carrera, A. Pagani, S. Valvano, Composites Part B: Engineering, **111**, 294 –314 (2017)
7. M.Y. Yasin, S. Kapuria, Composite Structures, **98**, 202–214 (2013)
8. M. Cinefra, E. Carrera, Int. J. Num. Meth. Eng. **93**, 2, 160-182 (2013)
9. M.F. Caliri, A. J.M. Ferreira, V. Tita, Composite Structures, **156**, 63–77 (2016)
10. V.I. Samul'. *Fundamentals of the Theory of Elasticity and Plasticity* (Vysshaya Shkola, Moscow, 1982)
11. A.D. Matveev, Vestnik Krasnoyarskogo Gosudarstvennogo Agrarnogo Universiteta, **3**, 44-47 (2014)
12. A.D. Matveev, A.N. Grishanov, Izvestia Altaiskogo Gosudarstvennogo Universiteta. Seriya: Matematika i Mekhanika, **4**, 120-125 (2017)

13. A. D. Matveev. *The Multigrid Finite Element Method in Calculating Three-Dimensional Homogeneous and Composite Solids*. Uchen. Zap. Kazan. Univ. Ser.: Fiz.-Matem. Nauki, **158**, No. 4, 530-543 (2016)
14. A.D. Matveev, Vestnik KrasGAU, **11**, 131-140 (2017)
15. A.D. Matveev, Vestnik KrasGAU, **2**, 90-103 (2018)
16. A.D. Matveev, Vestnik KrasGAU, **3**, 126-137 (2018)
17. A.D. Matveev, IOP Conf. Ser.: Mater. Sci. Eng. **158**, 1, 012067, 1-9 (2016)
18. A.D. Matveev, Vestnik KrasGAU, **6**, 141-154 (2018)
19. Y Xia, M.I. Friswell, E.I Saavedra Flores, Itern. J. Solids Structures **49**, 14, 1453-1462 (2012)
20. N. Talbi, A. Batti, R. Ayad, Y.Q. Guo, Composite Structures **88**, 280-289 (2009)